Energetics of Z-DNA binding protein-mediated helicity reversals in DNA, RNA, and DNA-RNA duplexes

ARTICLE *in* THE JOURNAL OF PHYSICAL CHEMISTRY B · OCTOBER 2013

Impact Factor: 3.3 · DOI: 10.1021/jp409862j · Source: PubMed

6 AUTHORS, INCLUDING:

Doyoun Kim
Institute for Basic Science
19 PUBLICATIONS **133** CITATIONS

SEE PROFILE

THE JOURNAL OF PHYSICAL CHEMISTRY B

Article

pubs.acs.org/JPCB

Energetics of Z-DNA Binding Protein-Mediated Helicity Reversals in DNA, RNA, and DNA−RNA Duplexes

Sangsu Bae,[†,‡,#] Yuyoung Kim,[†,‡] Doyoun Kim,[∥] Kyeong Kyu Kim,*[,∥] Yang-Gyun Kim,*[,⊥] and Sungchul Hohng*[,†,‡,§]

[†]Department of Physics and Astronomy, [‡]National Center for Creative Research Initiatives, and [§]Department of Biophysics and Chemical Biology, Seoul National University, Seoul 151-747, Korea

[∥]Department of Molecular Cell Biology, Samsung Biomedical Research Institute, Sungkyunkwan University School of Medicine, Suwon, Gyeonggi 440-746, Korea

[⊥]Department of Chemistry, Sungkyunkwan University, Suwon, Gyeonggi 440-746, Korea

Supporting Information

ABSTRACT: Z-DNA binding proteins (ZBPs) specifically recognize and stabilize left-handed double helices, including Z-DNA and Z-RNA. However, the energetics of Z-form stabilization by ZBPs have never been characterized due to the technical limitations of bulk studies, resulting in an unclear understanding of the ZBP operational mechanism at the molecular level. Here, we use single-molecule fluorescence resonance energy transfer (FRET) to determine the energetics of Z-form stabilization by ZBP for DNA, RNA, and DNA−RNA duplexes, revealing that the formation of B−Z or A−Z junctions dominates the thermodynamics and kinetics of Z-form stabilization. Furthermore, in contrast to general assumptions, the Z-form is most efficiently and most rapidly formed in the DNA−RNA hybrid duplex due to the greatly reduced junction energy in the DNA−RNA hybrid.

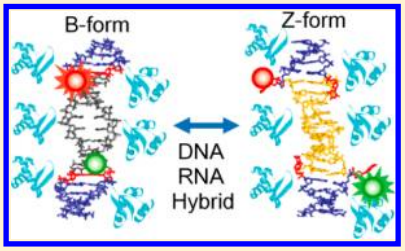

INTRODUCTION

Z-DNA, a left-handed isoform of Watson and Crick's right-handed B-DNA, is the first discovered oligonucleotide double helix with left helicity.[1] Its existence was first suggested in the circular dichroism measurements performed in high salt conditions.[2] The suspicion of handedness reversal between B-form and Z-form was subsequently confirmed via Raman spectroscopy and X-ray crystallography.[3,4] In particular, the atomic structure of Z-DNA revealed that in contrast to B-form, in which all bases are in an anticonformation, bases in Z-form alternate between syn- and anti-conformations, providing a natural explanation for why Z-DNA was preferentially formed in purine/pyrimidine repeats.[5,6] The syn-conformation is more easily formed in purines than in pyrimidines.

Various factors stabilize Z-DNA, such as the amount of bromination, chemicals, or multivalent cations.[7−9] In cells, methylation and negative supercoiling appear to stabilize Z-DNA.[10,11] The existence of Z-DNA-specific binding proteins (ZBPs) further signifies the biological implication of Z-DNA.[12] Purine−pyrimidine repeats are abundant in eukaryotic genomes (once every 3000 base pairs in the human genome) and are nonrandomly located in transcription initiation sites.[13,14] Therefore, it has been suggested that Z-DNAs play an important role in the regulation of gene transcription.[15] However, ZBPs play significant roles in many cellular functions: adenosine deaminase acting on RNA (ADAR1), a RNA-editing deaminase; DNA-dependent activator of IFN-regulatory factors (DAI), a cytosolic activator of the innate immune system; E3L, a virulence factor of the poxvirus family involved in the viral pathogenesis, etc.[16−20] Furthermore, it was discovered that ZBPs can also stabilize Z-form RNA.[21] These results suggest that not only the roles of ZBPs in cellular responses but also their natural substrates in cells may be diverse.

The detailed interactions between ZBPs and Z-form nucleic acids have been studied using various techniques, including X-ray crystallography and nuclear magnetic resonance (NMR).[22−25] However, current studies mostly provide structural aspects of the interactions. The energetics of ZBP-mediated Z-form stabilization have never been studied due to the lack of appropriate techniques, and as a result, the underlying mechanism of ZBP-mediated Z-form stabilization remains unclear.

In our ongoing effort to elucidate the mechanistic details of Z-DNA stabilization by ZBPs, we recently established a single-molecule fluorescence resonance energy transfer (FRET) assay to accurately quantitate Z-form formation in the DNA double helix.[26,27] Here, we extended the study to determine the energetics of ZBP-mediated Z-form stabilization for DNA, RNA, and DNA−RNA hybrid duplexes, revealing that the formation of B−Z or A−Z junctions is a dominating factor for the thermodynamics and kinetics of Z-form stabilization. Interestingly, Z-form was most rapidly and efficiently stabilized by ZBPs in the DNA−RNA hybrid due to the significant reduction of junction free energy.

Received: October 3, 2013
Revised: October 10, 2013
Published: October 10, 2013

MATERALS AND METHODS

Protein, DNA, RNA, and Hybrid Sample Preparation. Proteins were prepared as described.[23] DNA strands were purchased from Integrated DNA Technologies (Coralville, IA), and labeled with Cy3 or Cy5 as described.[28] DNA duplexes were formed by mixing the biotinylated and non-biotinylated strands in 1:2 ratio at 50 μM concentration in a buffer containing 10 mM Tris (pH 8.0) and 50 mM NaCl. The non-biotinylated strand was added in excess to minimize the chance of having an un-annealed biotinylated strand in the measurement. The annealing mixture was heated at 95 °C for 3 min and allowed to cool down slowly to room temperature for 1.5 h in a heating block. The RNA strands for R6 (Figure 1) were purchased from ST Pharm Co. (South Korea), and labeled with Cy3 or Cy5. The RNA strands for R8 (Figure 1) were purchased from Dharmacon Inc. (Lafayette, CO), and labeled with DY547 or DY647. RNA duplexes were prepared by using the same protocol as for DNA except that the annealing buffer contains additional 1 mM EDTA.

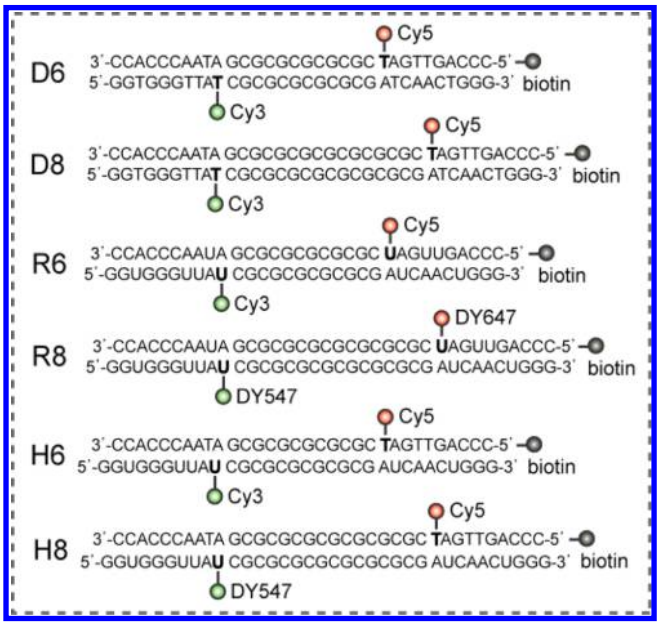

Figure 1. Design of DNA, RNA, and DNA–RNA duplexes for the experiments. Oligonucleotide sequences and modification sites are indicated for each sample.

Single-Molecule FRET Measurements. A quartz slide was coated with poly(ethylene glycol) (PEG, m-PEG-5000; Laysan Bio Inc.) and 1–2% biotinylated PEG (biotin-PEG-5000; Laysan Bio Inc.) as described.[28] After injecting streptavidin (Sigma, 0.2 mg/mL) into the channel and immobilizing biotinylated oligonucleotides (100 pM) via a biotin–streptavidin interaction on a polymer-coated surface, single-molecule fluorescence images were obtained in a wide-field total-internal-reflection fluorescence microscope with 100 ms time resolution using an electron multiplying charge-coupled device (EM-CCD) camera (iXon DV887ECS-BV, Andor Technology) and a homemade program written by Microsoft C++ program. Measurements were performed in an imaging buffer containing 10 mM Tris–HCl (pH 8.0), 50 mM NaCl, and an oxygen scavenger system to slow photobleaching: 2.5 mM PCA (Sigma-Aldrich), 50 nM PCD (Sigma-Aldrich), 1% (v/v) Trolox (Sigma-Aldrich).[29]

Bulk FRET Measurements. Bulk FRET efficiency was measured by using a Varian Eclipse fluorescence spectrophotometer. Oligonucleotide duplex (10 nM) was incubated in a buffer containing 10 mM Tris–HCl (pH 8.0) and 50 μM hZα_{ADAR1} at the designated temperature. The sample was excited at 500 nm, and emission fluorescence signals at 565 and 665 nm were measured for Cy3 and Cy5, respectively. FRET efficiency was calculated by $I_{665nm}/(I_{565nm} + I_{665nm})$, where I_{peak} means the fluorescence intensity at the peak wavelength.

Determination of Thermodynamic Parameters. To obtain the entropy and enthalpy of Z-form transition, equilibrium constants (K_{eq}) at varying temperatures (T) were fitted to the van't Hoff equation: $\ln(K_{eq}) = (\Delta S°/R) - (1/T)(\Delta H°/R)$, where R, $\Delta S°$, and $\Delta H°$ are the ideal gas constant, the transition entropy, and the transition enthalpy, respectively.[30] To obtain the enthalpic barriers of Z-form transition, we first determined the forward transition rate (k_f, the transition rate from non-Z-form to Z-form) and the backward transition rate (k_b, the transition rate from Z-form to non-Z-form) at each temperature by solving the following equations: $K_{eq} = (k_f/k_b)$ and $\tau^{-1} = k_f + k_b$, where τ is the kinetic time constant obtained from bulk FRET measurement. Then, temperature-dependent reaction rates (k: k_f or k_b) were fitted to the Arrhenius equation: $\ln(k) = A - (1/T)(\Delta H^{‡}/R)$, where A and $\Delta H^{‡}$ are a fitting constant and the enthalpic barrier of the transition, respectively.[30]

RESULTS

Z-Form of DNA–RNA Hybrid Is Most Efficiently Stabilized by ZBP. Because Z-form double-helical nucleic acids are preferably formed in purine–pyrimidine repeats, there is a high probability in a biological context that Z-form will be

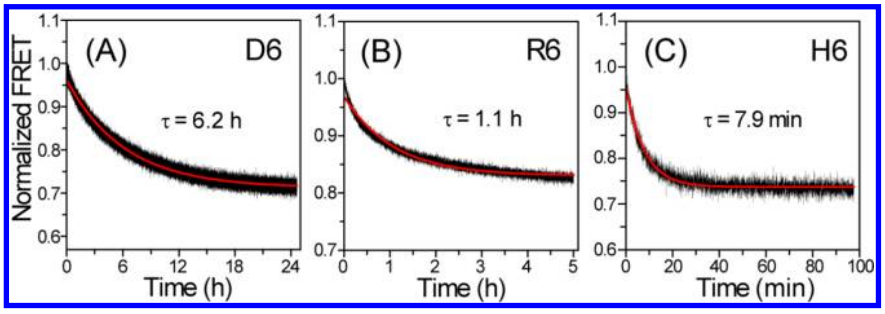

Figure 2. Comparison of Z-form transition kinetics of various nucleic acid duplexes by hZα_{ADAR1}. Bulk FRET time traces of D6 (A), R5 (B), and H6 (C) after adding 50 μM hZα_{ADAR1} are shown. The transition times were obtained by fitting the data to a single exponential function. (Adjusted R^2 is 0.981, 0.968, and 0.923, respectively).

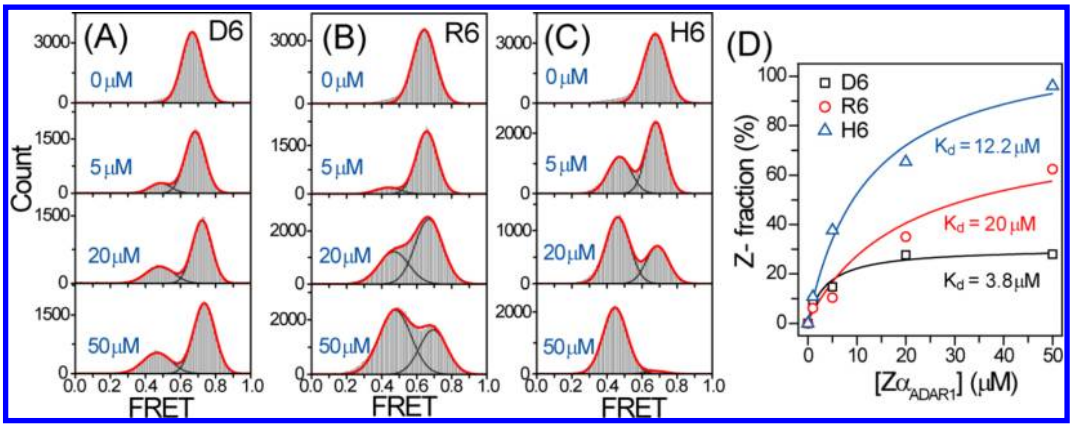

Figure 3. Comparison of Z-form stabilization efficiencies in DNA, RNA, and DNA–RNA duplexes. Single-molecule FRET histograms of D6 (A), R6 (B), and H6 (C) at varying hZα_{ADAR1} concentrations are shown. (D) Z-form population as a function of hZα_{ADAR1} concentration. The phenomenological dissociation constants of hZα_{ADAR1} (K_d) were obtained by fitting the data to a Hill equation (n = 1). All experiments were performed at 29 °C.

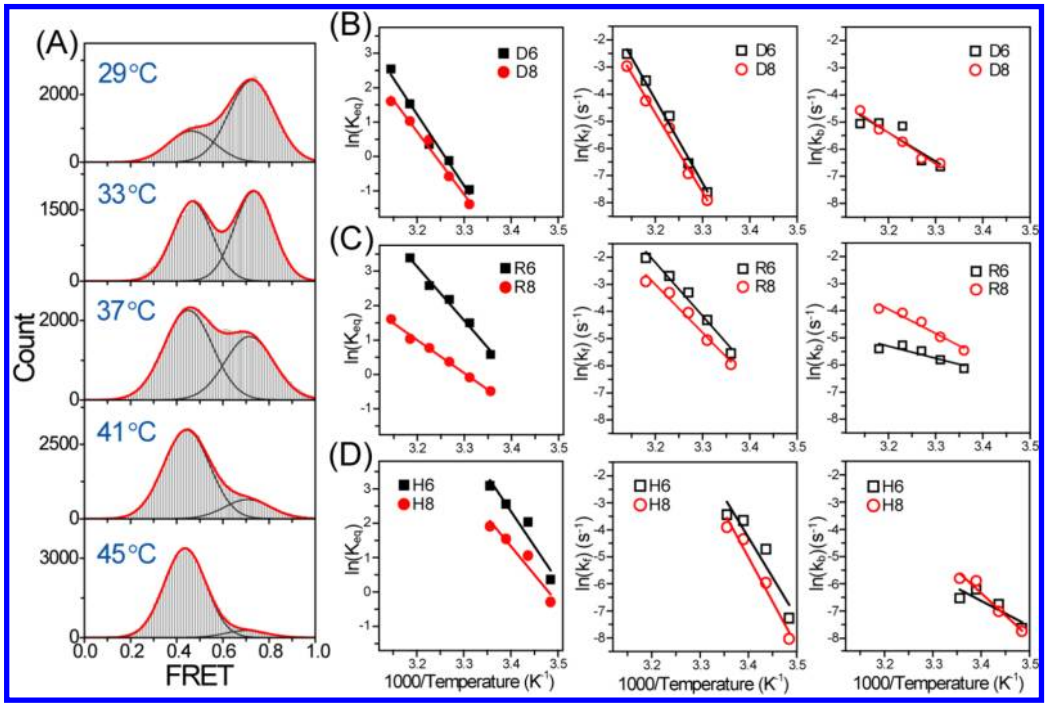

Figure 4. Temperature dependence of Z-form formation. (A) FRET histograms of D6 at varying temperatures ([hZα_{ADAR1}] = 50 μM). Temperature dependence of the Z-form equilibrium constant (left), the forward transition rate to Z-form (middle), and the backward transition rate from Z-form (right) for D6 and D8 (B), R6 and R8 (C), and H6 and H8 (D).

embedded in long stretches of non-Z-form nucleic acids, such as B-form dsDNA. With this in mind, we prepared dye-labeled DNA, RNA, and DNA–RNA hybrid duplexes that had CG repeats in the center with flanking random sequences (Figure 1). The thymine or uracil base at the Z-form and non-Z-form junction was selected as the labeling position for fluorophores to maximize FRET change during the Z-form stabilization,[23] and one end of each duplex was biotinylated for surface immobilization. Depending on the duplex composition (D for DNA, R for RNA, and H for hybrid) and the number of the central CG repeats (n), each sample was named as Dn, Rn, and Hn, respectively. For instance, D6 refers to a DNA duplex with six CG repeats at the center.

First, the kinetics of the Z-form stabilization were characterized with bulk FRET measurements. We determined how rapidly and efficiently the Z-form was stabilized by the Zα domain of human double-stranded RNA adenosine deaminase (hZα_{ADAR1}) in DNA, RNA, and hybrid duplexes. Parts A, B, and C in Figure 2 show the bulk FRET traces for D6, R6, and H6 after adding 50 μM hZα_{ADAR1} at 29 °C. The equilibrium in H6 is reached noticeably and significantly faster than that in R6 or D6. To quantitate the exact Z-form population at equilibrium, single-molecule FRET was performed. For single-molecule experiments, duplex oligonucleotides were immobilized on a polymer-coated quartz surface via streptavidin–biotin interaction and were incubated with varying concentrations of hZα_{ADAR1}. The incubation time was chosen on the basis of the time constants measured in Figure 2A–C to ensure that the Z-form transition equilibrium was established. Single-molecule images were obtained using a wide-field total-internal-reflection

dx.doi.org/10.1021/jp409862j | J. Phys. Chem. B 2013, 117, 13866–13871

Table 1. Thermodynamic Parameters Obtained from Figure 4

	$\Delta H°$ (kcal/mol)	$\Delta S°$ (cal/mol·K)	$\Delta G°$ [a] (kcal/mol)	$\Delta H_f^‡$ (kcal/mol)	$\Delta H_b^‡$ (kcal/mol)
D6	41.3 ± 3.5	134.5 ± 11.4	1.22	61.4 ± 3.6	20.2 ± 5.9
D8	36.3 ± 2.5	117.5 ± 8.1	1.29	59.9 ± 2.7	23.7 ± 2.2
R6	31.1 ± 2.1	105.8 ± 6.7	−0.43	39.2 ± 3.5	8.9 ± 2.6
R8	19.1 ± 0.8	63.1 ± 2.5	−0.30	35.3 ± 3.4	17.8 ± 2.3
H6	40.5 ± 7.7	142.4 ± 26.2	−1.94	47.5 ± 8.5	7.0 ± 4.8
H8	33.0 ± 6.2	114.8 ± 21.3	−1.21	49.5 ± 5.1	16.5 ± 9.0

[a]The Gibbs free energy ($\Delta G°$) was calculated at 25 °C by the definition $\Delta G° = \Delta H° - T\Delta S°$.

Table 2. Enthalpic and Entropic Contributions of the CG Repeat and the Junction to the Standard Free Energy Change of Z-Form Formation[a]

	DNA			RNA			hybrid		
	$\Delta H°$	$\Delta S°$	$\Delta G°$	$\Delta H°$	$\Delta S°$	$\Delta G°$	$\Delta H°$	$\Delta S°$	$\Delta G°$
(CG)	−2.5	−8.5	0.04	−6.0	−21.4	0.37	−3.8	−13.8	0.37
junction	28.2	92.8	−0.51	33.6	117.0	−1.31	31.5	112.6	−2.07

[a]The unit of $\Delta H°$ and $\Delta G°$ is kcal/mol, and the unit of $\Delta S°$ is cal/mol·K. The Gibbs free energy ($\Delta G°$) was calculated at 25 °C.

fluorescence microscope. Parts A, B, and C of Figure 3 show FRET histograms of D6, R6, and H6 incubated with the designated hZα_{ADAR1} concentrations. Circular dichroism (CD) measurements also confirmed Z-form stabilization of D6, R6, and H6 by hZα_{ADAR1} dependence (Figure S1 in the Supporting Information). As previously reported,[26,27] the low FRET state appearing at high hZα_{ADAR1} concentrations indicates the presence of Z-form. These single-molecule FRET histograms were fitted to a sum of two Gaussian functions, providing a way to accurately quantitate the Z-form population at equilibrium. This confirms that Z-form is most efficiently formed in H6, consistent with the observation in bulk FRET. However, there is no strong correlation between the phenomenological dissociation constants of hZα_{ADAR1} (K_d, the hZα_{ADAR1} concentration at which half of the saturated Z-form population is reached) and Z-form stabilization efficiencies (Figure 3D). Therefore, this rapid and efficient Z-form stabilization occurring in the DNA−RNA hybrid is not due to the high binding affinity of hZα_{ADAR1} to the hybrid duplex.

Z-Form Is Favored at Higher Temperatures. To further investigate the energetics of Z-form stabilization, we examined the temperature dependence of Z-form stabilization efficiencies and kinetics in the presence of the saturation concentration of hZα_{ADAR1} (50 μM). Figure 4A shows single-molecule FRET histograms of D6 at five different temperatures. Likewise, Z-form populations were measured at various temperatures for D8 (Figure S2, Supporting Information), R6 and R8 (Figure S3, Supporting Information), and H6 and H8 (Figure S4, Supporting Information). These results are summarized in Figure 4B−D. In all samples, the Z-form became more populated with increasing temperature (Figure 4B−D, left), indicating that ZBP-mediated Z-form stabilization is an endothermic process. The forward transition rates (k_f, the transition rate from A- or B-form to Z-form) and the backward transition rates (k_b, the transition rate from Z-form to A- or B-form) were determined from the equilibrium constants (Figure 4B−D) and the kinetic time constants (Figure S5−S7, Supporting Information). Because the equilibrium constant of Z-form stabilization obtained from the single-molecule FRET measurements provides a ratio between the forward rate and the backward rate, whereas the kinetic time constant of Z-form stabilization obtained in bulk FRET measurements as in Figure 2A−C provides the sum of the forward and backward rates, the two rates can be uniquely determined by combining the two relations. Both the forward rates (Figure 4B−D, middle) and the backward rates (Figure 4B−D, right) increased with temperature, indicating that enthalpic barriers exist for such conformational transitions.

DNA−RNA Hybrid Has the Lowest Junction Energy. Finally, we determined the thermodynamic parameters of Z-form stabilization by hZα_{ADAR1} (Table 1) by fitting the equilibrium constants of the Z-form/non-Z-form transitions with the van't Hoff equation or the transition rates with the Arrhenius equation (Materials and Methods). These thermodynamic functions were decomposed into the contributions of the junction part and the CG repeat part (Tables 2 and 3). Given that the Gibbs free energy contribution of each sample is composed of two components (the junction and the CG repeat), the thermodynamic functions of both the CG repeat and the junction could be determined from a pair of samples with the same duplex composition and different CG repeat numbers (e.g., H6 and H8 are divided into six and eight CG repeats with two junctions, respectively).

Table 3. Contributions of the CG Repeat and the Junction to the Enthalpic Barriers[a]

	DNA		RNA		hybrid	
	$\Delta H_f^‡$	$\Delta H_b^‡$	$\Delta H_f^‡$	$\Delta H_b^‡$	$\Delta H_f^‡$	$\Delta H_b^‡$
(CG)	−0.8	1.8	−2.0	4.5	1.0	4.8
junction	33.0	4.9	25.5	−9.0	20.8	−10.8

[a]The unit is kcal/mol for all.

DISCUSSION

On the basis of the numbers obtained from our study (Tables 1−3), the following conclusions were derived. First, it was previously reported that the transition free energy of the CG repeat for the intrinsic B-to-Z transition of the DNA duplex was +0.66 kcal/mol and that of the junction was +5.0 kcal/mol, as measured in supercoiled DNAs at room temperature.[31] Compared to these values, we found ZBPs greatly reduce both the CG repeat free energy (+0.04 kcal/mol) and the junction free energy (−0.51 kcal/mol) (Table 2) at room temperature. Therefore, ZBPs significantly contribute to the

dx.doi.org/10.1021/jp409862j | J. Phys. Chem. B 2013, 117, 13866−13871

stabilization of both the B−Z junction and the Z-form in the CG repeats. We previously showed that hZα_{ADAR1} stabilizes Z-DNA via the conformational selection mechanism.[26] Therefore, we would like to mention that all the effects of hZα_{ADAR1} observed in this work should be considered as being originated from selective interaction of the protein with transiently formed intrinsic Z-form structure.

Second, we found that the entropic term drove the transition to Z-form for all duplexes investigated in this study, while the enthalpic term hindered the transition (Table 1). Furthermore, when these energetic terms were decomposed into the junction part and the CG repeat part, the same entropy−enthalpy competition was observed for the junction part, while the opposite behavior was observed for the CG repeat part (Table 2). Therefore, the finding that ZBP-mediated Z-form stabilization is entropically driven is a natural consequence of the fact that the junction part dominates the overall energetics of the Z-form transition for short CG repeats. However, the question remains as to why the entropy of the junction part increases during Z-form stabilization. It is quite possible that the disruption of base pairings at the junctions between Z-form and non-Z-form duplexes may contribute to the increment of entropy.[23,25,32]

From our results, it is clear that Z-form stabilization in the DNA−RNA hybrid duplex was most rapidly (Figure 2) and efficiently completed (Figure 3). Its efficient Z-form transition is in good agreement with the preferable junction energy of the hybrid duplex (Table 2); i.e., the free energy cost of the CG repeat was compensated by the lowest free energy of the junction for the hybrid sample. Correspondingly, the swift Z-form stabilization in the hybrid duplex was achieved by the fact that the largest enthalpic barrier of the CG repeat is compensated by the smallest enthalpic barrier of the junction for the hybrid sample (Table 3). Therefore, Z-form transition occurs most easily in the hybrid duplex because its junction is preferable for Z-form formation.

Until now, despite a great deal of information about the in vitro and in vivo activities of ZBPs and considerable indirect evidence concerning their biological roles, the precise substrate(s) for ZBPs has not been clearly revealed. Our study elucidated that the DNA−RNA hybrid undergoes a conformational change to the Z-form by hZα_{ADAR1} with much more favorable kinetics than RNA and DNA duplexes. Thus, it is very intriguing to consider that the DNA−RNA hybrid may constitute one of the biologically relevant ligands that hZα_{ADAR1} and other ZBPs recognize and bind. Indeed, DNA−RNA hybrids occur throughout the cell in both the nucleus and cytosol and in many circumstances, such as RNA editing and viral pathogenesis. Additionally, short stretches of Z-forming sequences are prevalent in human and viral genomes.[33−36] Z-DNA binding domains present in various proteins may recognize such sequences and promote Z-form stabilization during the course of finding or reorganizing their target nucleic acid substrates. Thus, it is quite plausible that DNA−RNA hybrids may be one of the natural substrates for ZBPs, although the nature of the ligand(s) that they bind to remains to be determined—dsDNA, dsRNA, or DNA/RNA hybrid.

In summary, we determined the energetics of ZBP-mediated Z-form stabilization for DNA, RNA, and DNA−RNA duplexes with B−Z or A−Z junctions. From this in-depth analysis, the thermodynamic parameters for Z-form stabilization revealed that the energetic bottleneck for A-to-Z or B-to-Z transition in the duplex nucleic acids is the formation of junctions. Our experiments explored Z-form stabilization at sequences surrounded by either a right-handed B-form or A-form nucleic acid duplex. The junction regions not only contributed to easing the strain caused by opposite handedness occurring within a duplex but also consequently promoted swift conformational change toward Z-form. Our strategy could be extended to different sequence contexts containing CA/TG repeats and even non-purine/pyrimidine repeats other than CG repeats, which are more frequently present in potential Z-forming sequences. Future studies should explore different base pair compositions and lengths of Z-forming sequences to better understand Z-form formation in biological processes.

■ ASSOCIATED CONTENT

Supporting Information

Figures S1−S7 showing CD spectra, FRET histograms, and bulk FRET kinetic measurements. This material is available free of charge via the Internet at http://pubs.acs.org.

■ AUTHOR INFORMATION

Corresponding Authors

*E-mail: kyeongkyu@skku.edu (K.K.K).
*E-mail: ygkimmit@skku.edu (Y.-G.K).
*E-mail: shohng@snu.ac.kr (S.H.).

Present Address

#S.B.: Department of Chemistry, Seoul National University, Seoul 151-747, Korea.

Notes

The authors declare no competing financial interest.

■ ACKNOWLEDGMENTS

This work was supported by the Creative Research Initiatives (Physical Genetics Laboratory, 2009-0081562) and the World Class University program (R31-2009-100320) to S.H., the NRF international collaboration program (2011-0030915) and SBRI to K.K.K., and the Basic Science Research Program through the National Research Foundation of Korea (NRF), funded by the Ministry of Education, Science and Technology (2009-0075300) to Y.-G.K. S.B. was partly supported by the Seoul R&BD program.

■ REFERENCES

(1) Rich, A. DNA Comes in Many Forms. *Gene* **1993**, *135*, 99−109.
(2) Pohl, F. M.; Jovin, J. M. Salt-Induced Co-operative Conformational Change of a Synthetic DNA: Equilibrium and Kinetic Studies with Poly (dG-dC). *J. Mol. Biol.* **1972**, *67*, 375−396.
(3) Thamann, T. J.; Lord, R. C.; Wang, A. H. -J.; Rich, A. The High Salt Form of Poly(dG-dC)·Poly(dG-dC) Is Left-Handed Z-DNA: Raman Spectra of Crystals and Solutions. *Nucleic Acids Res.* **1981**, *9*, 5443−5457.
(4) Wang, A. H.-J.; Quigley, G. J.; Kolpak, F. J.; Crawford, J. L.; Van Boom, J. H.; Van Der Marel, G.; Rich, A. Molecular Structure of a Left-Handed Double Helical DNA Fragment at Atomic Resolution. *Nature* **1979**, *282*, 680−686.
(5) Haniford, D. B.; Pulleyblank, D. E. Facile Transition of Poly[d(TG)·d(CA)] into a Left-Handed Helix in Physiological Conditions. *Nature* **1983**, *302*, 632−634.
(6) Rich, A.; Nordheim, A.; Wang, A. H. -J. The Chemistry and Biology of Left-Handed Z-DNA. *Annu. Rev. Biochem.* **1984**, *53*, 197−846.
(7) Peck, L. J.; Nordheim, A.; Rich, A.; Wang, J. C. Flipping of Cloned d(pCpG)n·d(pCpG)n DNA Sequences From Right- to Left-Handed Helical Structure by Salt, Co(III), or Negative Supercoiling. *Proc. Natl. Acad. Sci. U.S.A.* **1982**, *79*, 4560−4564.

(8) Fuertes, M. A.; Cepeda, V.; Alonso, C.; Pérez, J. M. Molecular Mechanisms for the B−Z Transition in the Example of Poly[d(G-C)·d(G-C)] Polymers. A Critical Review. *Chem. Rev.* **2006**, *106*, 2045−2064.
(9) Wu, Z.; Tian, T.; Yu, J.; Weng, X.; Liu, Y.; Zhou, Z. Formation of Sequence-Independent Z-DNA Induced by a Ruthenium Complex at Low Salt Concentrations. *Angew. Chem., Int. Ed.* **2011**, *50*, 11962−11967.
(10) Behe, M.; Zimmerman, S.; Felsenfeld, G. Changes In the Helical Repeat of Poly(dG-m5dC)·Poly(dG-m5dC) and Poly(dG-dC)·Poly-(dG-dC) Associated with the B−Z Rransition. *Nature* **1981**, *293*, 233−235.
(11) Rahmouni, A. R.; Wells, R. D. Stabilization of Z-DNA in Vivo by Localized Supercoiling. *Science* **1989**, *246*, 358−363.
(12) Herbert, A.; Lowenhaupt, K.; Spitzner, J.; Rich, A. Chicken Double-Stranded RNA Adenosine Deaminase Has Apparent Specificity for Z-DNA. *Proc. Natl. Acad. Sci. U.S.A.* **1995**, *92*, 7550−7554.
(13) Hamada, H.; Kakunaga, T. Potential Z-DNA Forming Sequences Are Highly Dispersed in the Human Genome. *Nature* **1982**, *298*, 396−398.
(14) Schroth, G. P.; Chou, P. J.; Ho, P. S. Mapping Z-DNA in the Human Genome. Computer-Aided Mapping Reveals a Nonrandom Distribution of Potential Z-DNA-Forming Sequences in Human Genes. *J. Biol. Chem.* **1992**, *267*, 11846−11855.
(15) Rich, A.; Zhang, S. Z-DNA: The Long Road to Biological Function. *Nat. Rev. Genet.* **2003**, *4*, 566−572.
(16) Schwartz, T.; Behlke, J.; Lowenhaupt, K.; Heinemann, U.; Rich, A. Structure of the DLM-1-Z-DNA Complex Reveals a Conserved Family of Z-DNA-Binding Proteins. *Nat. Struct. Biol.* **2001**, *8*, 761−765.
(17) Rothenburg, S.; Deigendesch, N.; Dittmar, K.; Koch-Nolte, F.; Haag, F.; Lowenhaupt, K.; Rich, A. A PKR-Like Eukaryotic Initiation Factor 2α Kinase from Zebrafish Contains Z-DNA Binding Domains Instead of dsRNA Binding Domains. *Proc. Natl. Acad. Sci. U.S.A.* **2005**, *102*, 1602−1607.
(18) Kim, Y. -G.; Muralinath, M.; Brandt, T.; Pearcy, M.; Hauns, K.; Lowenhaupt, K.; Jacobs, B. L.; Rich, A. A Role for Z-DNA Binding in Vaccinia Virus Pathogenesis. *Proc. Natl. Acad. Sci. U.S.A.* **2003**, *100*, 6974−6979.
(19) Ha, S. C.; Lokanath, N. K.; Van Quyen, D.; Wu, C. A.; Lowenhaupt, K.; Rich, A.; Kim, Y. -G.; Kim, K. K. A Poxvirus Protein Forms a Complex with Left-Handed Z-DNA: Crystal Structure of a Yatapoxvirus Zα Bound to DNA. *Proc. Natl. Acad. Sci. U.S.A.* **2004**, *101*, 14367−14372.
(20) Takaoka, A.; Wang, Z.; Choi, M. K.; Yanai, H.; Negishi, H.; Ban, T.; Lu, Y.; Miyagishi, M.; Kodama, T.; Honda, K.; et al. DAI (DLM-1/ZBP1) is a Cytosolic DNA Sensor and an Activator of Innate Immune Response. *Nature* **2007**, *448*, 501−505.
(21) Brown, B. A., II; Lowenhaupt, K.; Wilbert, C. M.; Hanlon, E. B.; Rich, A. The Zα Domain of the Editing Enzyme dsRNA Adenosine Deaminase Binds Left-Handed Z-RNA as well as Z-DNA. *Proc. Natl. Acad. Sci. U.S.A.* **2000**, *97*, 13532−13586.
(22) Schwartz, T.; Rould, M. A.; Lowenhaupt, K.; Herbert, A.; Rich, A. Crystal Structure of the Zα Domain of the Human Editing Enzyme ADAR1 Bound to Left-Handed Z-DNA. *Science* **1999**, *284*, 1841−1845.
(23) Ha, S. C.; Lowenhaupt, K.; Rich, A.; Kim, Y. -G.; Kim, K. K. Crystal Structure of a Junction between B-DNA and Z-DNA Reveals Two Extruded Bases. *Nature* **2005**, *437*, 1183−1186.
(24) Lee, Y. -M; Kim, H. -E.; Park, C. -J.; Lee, A. -R.; Ahn, H. -C.; Cho, S. J.; Choi, K. -H.; Choi, B. -S.; Lee, J. -H. NMR Study on the B−Z Junction Formation of DNA Duplexes Induced by Z-DNA Binding Domain of Human ADAR1. *J. Am. Chem. Soc.* **2012**, *134*, 5276−5283.
(25) Bothe, J. R.; Lowenhaupt, K.; Al-Hashimi, H. M. Sequence-Specific B-DNA Flexibility Modulates Z-DNA Formation. *J. Am. Chem. Soc.* **2011**, *133*, 2016−2018.
(26) Bae, S.; Kim, D.; Kim, K. K.; Kim, Y. -G.; Hohng, S. Intrinsic Z-DNA Is Stabilized by the Conformational Selection Mechanism of Z-DNA-Binding Proteins. *J. Am. Chem. Soc.* **2011**, *133*, 668−671.
(27) Bae, S.; Son, H.; Kim, Y. -G.; Hohng, S. Z-DNA Stabilization Is Dominated by the Hofmeister Effect. *Phys. Chem. Chem. Phys.* **2013**, *15*, 15829−15832.
(28) Roy, R.; Hohng, S.; Ha, T. A Practical Guide to Single-Molecule FRET. *Nat. Methods* **2008**, *5*, 507−516.
(29) Shi, X.; Lim, J.; Ha, T. Acidification of the Oxygen Scavenging System in Single-Molecule Fluorescence Studies: In Situ Sensing with a Ratiometric Dual-Emission Probe. *Anal. Chem.* **2010**, *82*, 6132−6138.
(30) Hanggi, P.; Talkner, P.; Borkovec, M. Reaction-Rate Theory: 50 Years after Kramers. *Rev. Mod. Phys.* **1990**, *62*, 251−341.
(31) Peck, L. J.; Wang, J. C. Energetics of B-to-Z Transition in DNA. *Proc. Natl. Acad. Sci. U.S.A.* **1983**, *80*, 6206−6210.
(32) Kim, D.; Reddy, S.; Kim, D. Y.; Rich, A.; Lee, S.; Kim, K. K.; Kim, Y. −G. Base Extrusion Is Found at Helical Junctions between Right- and Left-Handed Forms of DNA and RNA. *Nucleic Acids Res.* **2009**, *37*, 4353−4359.
(33) Zhang, L.; Kasif, S.; Cantor, C. R.; Broude, N. E. GC/AT-Content Spikes as Genomic Punctuation Marks. *Proc. Natl. Acad. Sci. U.S.A.* **2004**, *101*, 16855−16860.
(34) Khuu, P.; Sandor, M.; Deyoung, J.; Ho, P. S. Phylogenomic Analysis of the Emergence of GC-Rich Transcription Elements. *Proc. Natl. Acad. Sci. U.S.A.* **2007**, *104*, 16528−16533.
(35) Li, H.; Xiao, J.; Li, J.; Lu, L.; Feng, S.; Dröge, P. Human Genomic Z-DNA Segments Probed by the Zα Domain of ADAR1. *Nucleic Acids Res.* **2009**, *37*, 2737−2746.
(36) Cer, R. Z.; Bruce, K. H.; Mudunuri, U. S.; Yi, M.; Volfovsky, N.; Luke, B. T.; Bacolla, A.; Collins, J. R.; Stephens, R. M.; Non-B, D. B. A Database of Predicted Non-B DNA-Forming Motifs in Mammalian Genomes. *Nucleic Acids Res.* **2011**, *39*, D383−D391.